

# An Analytical Approach to the Design of Energy Harvesting Wireless Sensor Nodes

Shenqiu Zhang, *Student Member, IEEE*, Alireza Seyedi, *Senior Member, IEEE*,  
and Biplab Sikdar, *Senior Member, IEEE*

**Abstract**—Energy harvesting is one of the promising solutions to the problem of limited battery capacity in many wireless devices. This paper addresses the problem of system design of energy harvesting capable wireless devices in terms of the required sizes for energy and data buffers, as well as the size of the harvester, for given delay and loss requirements. We analyze the performance of an energy harvesting node, considering a stochastic model that takes into account energy harvesting and event arrival processes. We derive closed-form expressions for the probability of event loss and the average queueing delay. Our event-driven continuous time simulations validate our analytical results. Employing these results, we provide a near-optimal approach to the design of the system in terms of sizing the energy harvesting device, the energy storage, and the event queue capacity.

**Index Terms**—Energy harvesting, wireless sensor networks, rechargeable sensors, probability of loss, average delay.

## I. INTRODUCTION

THE popularity of small, battery operated wireless nodes, particularly wireless sensor nodes [1], has focused the attention of the research community on the issue of scarcity of energy. The problem arises from the desire for the wireless sensor nodes to be untethered and small, while having long operational lifetime [2]. The current and projected available energy density promised by the battery technology is not adequate to satisfy all these desirables at the same time [3]. Although a plethora of energy-efficient communication methods and protocols have been developed, e.g. [4]–[6], the problem is still far from being solved.

Energy harvesting, where the nodes harvest energy from ambient sources such as light, wind, water flow or human motion, is an attractive solution to the energy problem [7]. However, the majority of harvestable energy sources are stochastic in nature. Consequently, stochastic models and analysis must be used to study the performance of energy harvesting communication systems and to design new techniques that consider randomness of the energy source while optimizing system performance.

Recent attention to this subject has led to the development of a growing body of work. These works consider joint power and resource management problems ranging from source-channel

coding [8], [9], to node activation [10], [11], to scheduling and routing [12]–[15], to energy management [16]–[19]. However, little attention has been paid to the design of an energy harvesting node in terms of determining the required energy storage capacity, event queue capacity, and size of the energy harvesting device.

### A. Related Work

In this section we briefly review the existing work that have considered some aspects of the design problem. A power management scheme and an approach to the design of energy storage capacity are developed in [20]. In this work, a day is decomposed into many time slots. It is assumed that in each time slot, the harvesting power and the consumed power are constant and known. In [21], a scheduling scheme for power consumption is developed assuming a deterministic energy arrival process. The goal is to avoid empty or overflowing energy storage. With similar assumptions, i.e. deterministic harvested energy and consumed energy, [22] maximizes the amount of data transmitted by a deadline. In practice, however, the majority of ambient energy sources exploited for energy harvesting, as well as the energy consumption at the load are unpredictable and random in nature. Thus, one needs to consider the stochastic variations of these energy processes in order to develop more realistic performance characteristics and design approaches.

The work in [23] takes a step in this direction. The authors model energy harvesting and energy consumption as two independent bounded random processes. Given the minima and the maxima of the harvested energy and the energy consumption processes, a power management scheme is provided to ensure that the energy harvesting sensor node never runs out of energy [24]. However, in general the minima and the maxima do not adequately describe the stochastic nature of the energy harvesting or consumption processes. Moreover, the design goal of strictly guaranteeing a non-empty energy storage is only possible if the stochastic model is bounded, and often leads to a significant over-design of the system. It would be much more efficient to allow event loss and delay, with carefully set tolerance limits.

In [25], the authors take an empirical approach to design energy harvesting sensor nodes, in which the capacity of energy storages and the capability of harvesting devices are chosen based on the historical record of harvesting power [26] and predefined power consumption characteristics. Although the design approach does consider the actual variations of

S. Zhang is with the ECE Dept., University of Rochester, Rochester, NY, e-mail: shenqiu.zhang@rochester.edu, A. Seyedi is with the EECS Dept., University of Central Florida, Orlando, FL, email: alireza.seyedi@ieee.org, B. Sikdar is with the ECSE Dept., Rensselaer Polytechnic Institute, Troy, NY, email: sikdab@rpi.edu

This work has been funded in part by the National Science Foundation (NSF) grant CNS-1049691.

the energy harvesting process, it is time-consuming, highly dependent on the particular data set, and does not provide any insight into the effects of different parameters on the performance.

### B. Our contribution

In this paper, we analyze the performance of an energy harvesting node in terms of the probability of event loss and the average event queueing delay, in terms of the parameters of the energy harvesting and event arrival stochastic processes, and the parameters of the system, namely the size of the energy harvester (which affects the rate at which the device harvests energy) and the capacities of the event queue and the energy storage device. To this end, we employ a Markov model that unifies models of the energy process, the event arrival process, the energy storage and the queueing of events. We then use the derived closed-form expressions for the probability of event loss and the average delay to provide a near-optimal system design, in terms of sizing the energy storage, the queue capacity and the energy harvesting devices, given the tolerable levels of loss and delay.

Compared to our previous work in [27], the model and the analysis are generalized to remove the limiting assumptions on the system parameters. Moreover, the system set up has been extended to include the queueing of events. The analysis of average delay and the design methodology, given tolerable performance metrics, have also been added. Our simulations have also been updated to consider random channel access and the time it takes to process one event.

The remainder of the paper is organized as follows. Section II describes the system model. Sections III and IV provide the analysis of the probability of event loss and the average delay, respectively. Section V uses these results to perform a near-optimal design of the system parameters. Section VI presents the simulation results. Section VII concludes the paper. For readers' convenience, Table I lists the variables used, except for auxiliary variables and indices.

## II. MARKOVIAN MODEL FOR ENERGY HARVESTING NODES

### A. Model Assumptions

To model the behavior of an energy harvesting node, one needs to consider both energy harvesting and event arrival processes. A very popular model for the event arrival is the Poisson process. In other words, the event arrival process is often assumed to be Markovian. Many researchers also assume a Markovian model for analytical studies of the energy process [28]–[30]. Although particular sources may not be Markovian, the Markovian assumption provides a first order approximation in terms of the time dependence of the energy process, while maintaining mathematical tractability. Here we provide a unified Markov model for an energy harvesting node that describes the energy harvesting process, the energy consumption process, the amount of energy stored in the node and the queueing of events.

TABLE I: Variables used

Variable	Equals	Description	Unit
$\rho$		Harvesting power in active state	W
$E$		Energy consumed by one event	J
$T$		Time unit used in discretization	s
$k$	$\frac{E}{\rho T}$	Number of time units required to harvest energy for one event	-
$B$		Energy storage capacity	J
$N$	$\frac{B}{E}$	Energy storage capacity	events
$L$		Queue capacity	events
$\mu_a$		Rate of transition from active to inactive state	Hz
$\mu_i$		Rate of transition from inactive to active state	Hz
$\mu_e$		Rate of event arrival	Hz
$\eta$	$\frac{\mu_i \rho}{(\mu_i + \mu_a) \mu_e E}$	Ratio of average harvestable power to the average required power	-
$r$	$\approx \mu_a T$	Transition probability from active to inactive state	-
$w$	$\approx \mu_i T$	Transition probability from inactive to active state	-
$p$	$\approx \mu_e T$	Probability of event arrival in one time unit	-
$\mathbf{P}$	$[p_{i,j}]$	Transition probability matrix for the original Markov chain	-
$\boldsymbol{\pi}$	$[\pi_i]$	Steady state probability distribution for the original Markov chain	-
$\mathbf{Q}$	$[q_{i,j}]$	Transition probability matrix for the approximate Markov chain	-
$\tilde{\boldsymbol{\pi}}$	$[\tilde{\pi}_i]$	Steady state probability distribution for the approximate Markov chain	-
$P_k$		Probability of event loss (with $k$ discretization)	-
$\tilde{P}_k$		Approximate probability of event loss (with $k$ discretization)	-
$\tilde{P}$	$\lim_{k \rightarrow \infty} \tilde{P}_k$	Approximate probability of event loss	-
$\tilde{D}$		Approximate average event delay	s
$P_t$		Tolerable probability of event loss	-
$D_t$		Tolerable average event delay	s
$\alpha$		Unit cost per energy storage unit	\$/event
$\beta$		Unit cost per queue unit	\$/event
$\gamma$		Unit cost per harvesting device	\$/W
$C$		Total cost of an energy harvesting node	\$
$T_{\text{idle}}$		Average channel idle time	s
$T_{\text{busy}}$		Average channel busy time	s

1) *Harvesting Process*: We assume a two-state<sup>1</sup> harvesting source (*active* and *inactive*). The node collects energy at rate

<sup>1</sup>Although some literature assume multiple states for the harvesting process (e.g. [28]), this approach results in a large number of overall states, which renders the analysis intractable. Hence, we limit ourselves to two states, which is a common assumption in the literature [31]. The two-state energy model is a good approximation for describing many harvesting sources. For example, harvesting from human motion in a body area network where the subject is either in *rest* or *moving* states, or solar harvesting where the harvester may be *shaded/cloudy* or *clear*. Extension of our model and approach to a multi-state source is straightforward, though tedious.

(power)  $\rho$  in the active state and does not collect any energy in the inactive state. Following the Markovian assumption, we model the time durations for which the source stays in active and inactive states with independent exponential distributions with parameters  $\mu_a$  and  $\mu_i$ , respectively. The harvested energy is stored in an energy storage device (i.e. rechargeable battery or a super-capacitor), with capacity  $B$ . Any inefficiency in the charge and discharge process can be absorbed in the energy consumption model. Another imperfection of the storage devices can be energy leakage. While some works (e.g. [17]) do take this into account, here we assume that the energy storage device is perfect in terms of leakage, as it is commonly assumed in the literature [28]–[32]. In most cases, this is a reasonable assumption, since the leakage is only a secondary effect.

2) *Event Arrival Process*: We abstract the energy consumption process into *events* which include data transmission, as well as sensing and signal processing. We also assume that the inter-arrival times of the events are independent and exponentially distributed with parameter  $\mu_e$ . We further assume that there are no batch arrivals, which is a reasonable assumption for sensor networks. Arrived events enter a queue with capacity to store  $L$  events, and are served on a first-come-first-serve basis. If an event finds the queue to be full upon its arrival, it will be lost.

Events in sensor network correspond to measurements, observations, and data collected with reference to the application of interest. In typical scenarios such as environmental monitoring, surveillance, target tracking etc., the data generated in response to an event (i.e. an instance of a measurement/monitoring etc.) is fixed and the computations and operations required to gather and process the data at the sensor are also fixed [33], [34]. Thus we assume that each event generates a constant amount of data to be transmitted, and consumes a fixed amount of energy.

3) *Event Processing*: An event is processed when sufficient energy is available, consuming energy  $E$ . We assume that the energy storage device capacity,  $B$ , is sufficient for  $N$  events, i.e.  $B = NE$ . In our analytical approach we assume that the energy for processing an event is instantaneously removed from the energy storage device, as soon as there is sufficient energy. Of course, in reality processing of one event takes a finite amount of time, which is dominated by the transmission time. However, this transmission time, typically, is considerably smaller than the time required for harvesting sufficient energy for one event. For example, a MICAz mote requires 4.73mJ for transmitting a 132B packet (see Section VI) and thus requires 2.37 seconds for a solar energy harvester with a conversion rate of 2mW to generate sufficient energy for transmitting one packet. On the other hand, protocols such as IEEE 802.11 and IEEE 802.15.4 require only few tens of milliseconds for channel access even under saturated traffic conditions for moderate network sizes [35], [36]. Therefore, this assumption does not result in a noticeable deviation in the results.

The assumption that an event is served as soon as sufficient energy is available, implicitly assumes that the node is always able to access the channel. This also is not a bad assumption

for wireless sensor networks, which are often energy constrained, but are not expected to be bandwidth constrained. In Section VI, we compare our analytical results to those of simulations incorporating stochastic channel access to examine the acceptability of this assumption, as the channel access becomes more difficult.

### B. Discretized Model

We approach the analysis of the described continuous-time Markov model above, through discretization. We first discretize the time with a time unit  $T$ . This reduces our model to a discrete-time Markov model, which we analyze. Once the expressions for the desired performance metrics are at hand, we will consider them at the limit  $T \rightarrow 0$ . In other words, we obtain the performance of the continuous-time system by making the discretization steps infinitely small.

If  $T$  is sufficiently small, we have  $\mu_a T, \mu_i T \ll 1$ , with high probability. Consequently, the transition between the two harvesting states happens at most once during  $T$ . We denote the transition probability from active to inactive and vice versa within one time unit by  $r = \mu_a T e^{-\mu_a T} \approx \mu_a T$  and  $w = \mu_i T e^{-\mu_i T} \approx \mu_i T$ , respectively. Similarly, if  $\mu_e T \ll 1$ , no more than one event arrives during  $T$  and the probability of an event arriving in  $T$  is  $p = \mu_e T e^{-\mu_e T} \approx \mu_e T$ .

Define  $k = E/(\rho T)$ . This means that the node needs to stay in the active state for  $k$  time slots to harvest sufficient energy for one event. Thus, the capacity of the energy storage device is  $B = Nk\rho T$ . In other words, the storage device has the capacity of holding  $Nk$  units of energy, where a unit of energy is defined as  $\rho T = E/k$ . Also note that given  $\rho$  and  $E$ , the limits  $T \rightarrow 0$  and  $k \rightarrow \infty$  are equivalent.

The overall state of an energy harvesting node is determined by the remaining energy in the storage, the number of events in the queue and the harvesting state. Since events are processed as soon as sufficient energy is available, the queue length will be non-zero only if the stored energy is less than  $E$ . Similarly, the amount of stored energy will be no less than  $E$ , only if the queue is empty. With these two observations, we can consider an event waiting in the queue as *negative energy* stored (or energy owed). Therefore, a Markov chain with its states depicted in two dimensions (one for harvesting state and one for energy stored and queue length) is appropriate for describing a harvesting node (see Fig. 1 for an example with  $k = 3$ ). In other words, the state space is  $\{(m, s) | m \in \{-kL, \dots, kN\}$  and  $s \in \{0, 1\}\}$ . Index  $m$  represents the stored energy<sup>2</sup>. In other words, the amount of stored energy and the number of events in the queue are given by

$$E(m) = \begin{cases} \frac{m}{k} E & m \geq 0 \\ (\frac{m}{k} + \lceil -\frac{m}{k} \rceil) E & m < 0 \end{cases}$$

and

$$Q(m) = \begin{cases} 0 & m \geq 0 \\ \lceil -\frac{m}{k} \rceil & m < 0 \end{cases},$$

<sup>2</sup>From here on, unless otherwise stated, we use the generalized notion of *energy* (possibly negative) to describe the remaining actual energy and the queue length.

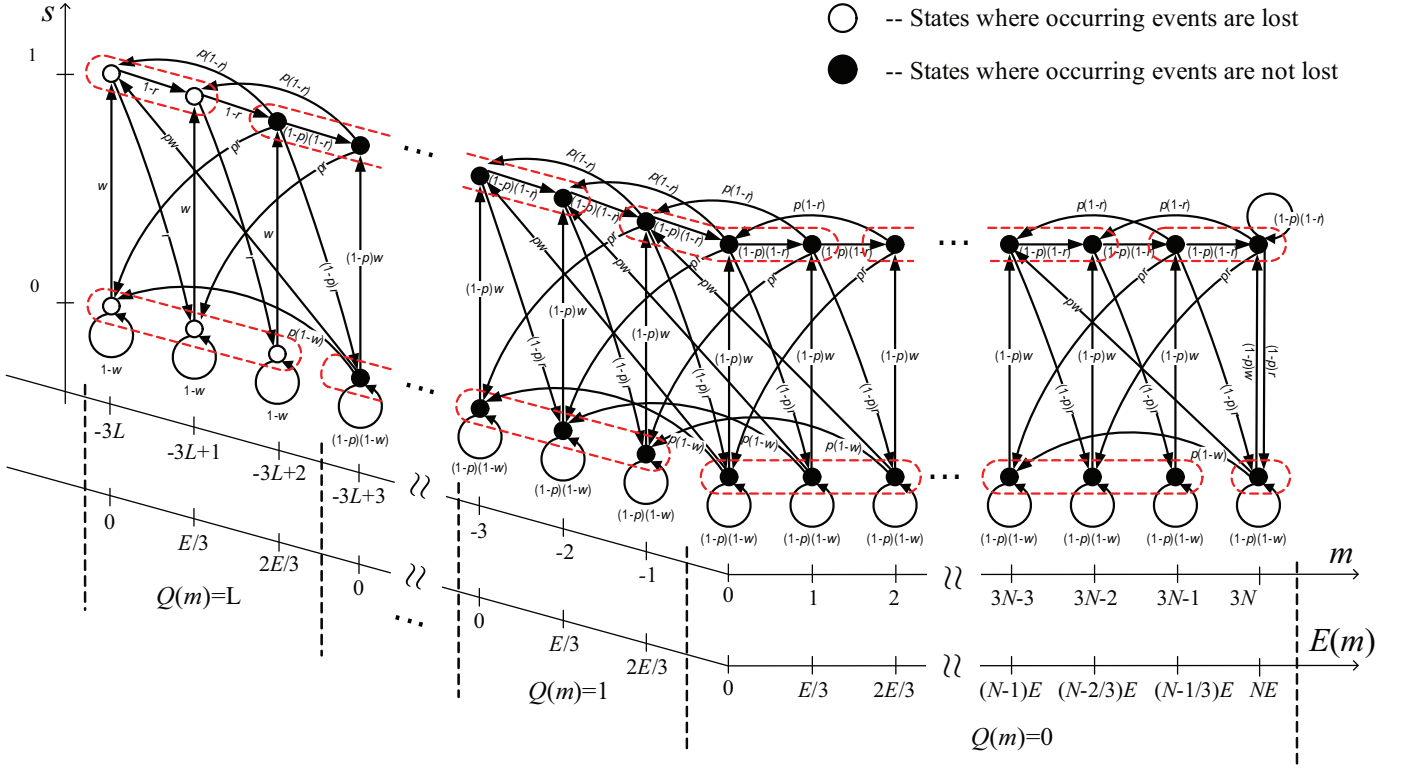


Fig. 1: Markov model of energy-harvesting sensors with a queue ( $k = 3$ ).

respectively. Inactive and active harvesting states are indexed with  $s = 0$  and  $s = 1$ , respectively. Although this indexing is more descriptive, we need to re-index the states by  $i = 2(m + kL) + s$  for vector and matrix notation.

Let  $\mathbf{P} = [p_{i,j}]$  be the transition matrix of the Markov chain, where  $p_{i,j}$  is the transition probability from the state  $i$  to the state  $j$ . We note the following transitions: (i) if a node is active, it will remain active with probability  $1 - r$  and will become inactive with probability  $r$ ; (ii) if a node is inactive, it will remain inactive with probability  $1 - w$  and will become active with probability  $w$ ; (iii) the node gains one energy unit if it is active, unless the storage is full; (iv) the node loses  $k$  energy units with probability  $p$ , unless no new events occur or the queue is full. To summarize, we have the following transition probabilities: For inactive states we have

$$p_{i < 2k, j} = \begin{cases} 1 - w & j = i \\ w & j = i + 1 \\ 0 & \text{otherwise} \end{cases} \quad (1)$$

and

$$p_{i \geq 2k, j} = \begin{cases} (1 - w)(1 - p) & j = i \\ (1 - w)p & j = i - 2k \\ w(1 - p) & j = i + 1 \\ wp & j = i - 2k + 1 \\ 0 & \text{otherwise} \end{cases} \quad (2)$$

and for active states we have

$$p_{i < 2k - 1, j} = \begin{cases} 1 - r & j = i + 2 \\ r & j = i + 1 \\ 0 & \text{otherwise} \end{cases}, \quad (3)$$

$$p_{2k - 1 \leq i \leq 2k(N + L), j} = \begin{cases} (1 - r)p & j = i - 2k + 2 \\ (1 - r)(1 - p) & j = i + 2 \\ rp & j = i - 2k + 1 \\ r(1 - p) & j = i + 1 \\ 0 & \text{otherwise} \end{cases} \quad (4)$$

and

$$p_{i = 2k(N + L) + 1, j} = \begin{cases} (1 - r)p & j = i - 2k + 2 \\ (1 - r)(1 - p) & j = i \\ rp & j = i - 2k + 1 \\ r(1 - p) & i = i - 1 \\ 0 & \text{otherwise} \end{cases} \quad (5)$$

In Fig. 1, the states that have a full queue and will lose incoming events, i.e. the inactive states  $2(m + kL)$  for  $-Lk \leq m \leq -Lk + k - 1$  and the active states  $2(m + kL) + 1$  for  $-Lk \leq m \leq -Lk + k - 2$ , are marked by hollow circles, while the remaining states (with sufficient queue space to store at least one more event) are marked by solid circles.

### III. EVENT LOSS PROBABILITY

It is easy to verify that the Markov chain defined in Section II is finite, irreducible and positive recurrent. Hence, it has a unique steady-state distribution,  $\boldsymbol{\pi} = [\pi_0, \dots, \pi_{2k(N+L)+1}]^T$ , where  $\pi_i$  is the steady-state probability of state  $i$ . Then, the probability of event loss due to queue overflow is<sup>3</sup>

$$P_k = \sum_{i=0}^{2k-2} \pi_i.$$

<sup>3</sup>We use the subscript  $k$  to remind us that we have discretized the initial model using the time unit  $T = E/(\rho k)$ .

Eigen analysis of the transition matrix  $\mathbf{P}$  can provide  $\pi$ , from which  $P_k$  can be obtained. However, in addition to the high degree of computational complexity, this numerical approach fails to provide us with any insight into how the system parameters affect its performance. In this section, we take an analytical approach and provide closed-form approximations of the probability of event loss.

#### A. Event Loss Probability with $L = 0$ and $k = 1$

Let us first examine the simple case where  $L = 0$  and  $k = 1$ , developed in [37].  $L = 0$  means that the events are not queued and  $k = 1$  implies that we have selected the time unit  $T$  such that the energy harvested in one time unit in the active state,  $\rho T$ , is equal to the energy required to process one event,  $E$ . Recall that we assume at most one event and at most one transition between active and inactive states take place in one time unit. This is a good approximation when  $\mu_a, \mu_i, \mu_e \ll \rho/E$ .

Let  $\eta$  be the ratio of average harvestable power,  $\frac{\mu_i \rho}{\mu_i + \mu_a}$ , to the average required power  $\mu_e E$ ,

$$\eta = \frac{\mu_i \rho}{(\mu_i + \mu_a) \mu_e E}. \quad (6)$$

Then, the exact closed-form expression for the probability of event loss in this case is [37]

$$P_{k=1, L=0} = \begin{cases} \frac{1-\eta}{1 - \frac{\mu_i}{\mu_a} \left( \frac{\rho}{\mu_e E} - 1 \right) \left[ 1 - \frac{\frac{\rho}{\mu_e E}}{1 + \left( \frac{\rho}{\mu_e E} - 1 \right) \frac{\mu_e}{\mu_i} \frac{\eta}{1-\eta}} \right]^N} & \eta \neq 1 \\ \frac{\mu_a}{\mu_i + \mu_a} \frac{1}{\eta + \frac{\mu_i}{\mu_e}} & \eta = 1 \end{cases} \quad (7)$$

It is easy to verify that (7) is a continuous function of  $\eta$ . An interesting point is  $\eta = 1$ . This is the *balanced point* where the average harvestable and required powers are equal. When  $\eta < 1$ , on average the load requires more energy than the source may possibly harvest, i.e. the node is *under-resourced*. When  $\eta > 1$ , on average the load requires less energy than the source can possibly harvest, i.e. the node is *over-resourced*.

A simple corollary of (7) can demonstrate the expected result when energy storage is large:

$$\lim_{N \rightarrow \infty} P_{k=1, L=0} = \begin{cases} 1 - \eta & \eta < 1 \\ 0 & \eta > 1 \end{cases}. \quad (8)$$

We see that in the over-resourced region the probability of event loss approaches zero, while in the under-resourced region, the probability of event loss is equal to  $1 - \eta$ , since no energy will be lost due to the energy storage device being infinitely large.

#### B. Event Loss Probability for General $L$ and $k$

The previous section recalled the exact closed-form expression for  $P_k$  when  $k = 1$  and  $L = 0$ . However, this is a good approximation only if  $\mu_a, \mu_i, \mu_e \ll \rho/E$ . When these conditions do not hold, we must use the general model with a large  $k$  to ensure that the time unit,  $T$ , is sufficiently small. Unfortunately, obtaining an exact closed-form solution for the Markov model with a large  $k$  is not tractable. Therefore, we resort to an approximation of the Markov model and a corresponding closed-form solution of the probability of event loss. To this end, we simplify the Markov model by merging a number of adjacent states with the same energy harvesting state (Fig. 1). This approximation is based on the observation that the adjacent states that have the same harvesting state have almost the same steady-state probabilities.

Using this approximation approach, we can approximate the probability of event loss with. See Appendix A for detailed derivations and definitions of the auxiliary variables  $s_k$ ,  $\delta_k$ ,  $\lambda_{i,k}$ ,  $g_{i,k}$ , and  $u_{i,k}$ .

Recall that (7) gives the exact probability of event loss for the original Markov chain with  $k = 1$  and  $L = 0$ . Next, we compare the approximated  $\tilde{P}_k$  and the exact  $P_{k=1, L=0}$ . Substituting  $k = 1$  and  $L = 0$  in (9) yields (10). Comparing (10) and (7), we can see that the  $P_{k=1, L=0}$  differs from  $\tilde{P}_{k=1, L=0}$  only in the term  $\left[ 1 - \frac{\mu_i E}{\rho} + \frac{\mu_a E}{\rho \left( \frac{\rho}{\mu_e E} - 1 \right)} \right]^2$  in the denominator, which vanishes if  $\mu_a, \mu_i, \mu_e \ll \rho/E$ .

If the assumption  $\mu_a, \mu_i, \mu_e \ll \rho/E$  is not satisfied, the parameter  $k$  has to be large enough in order to obtain a small time unit  $T$ . Thus, to obtain a more accurate model we make the time unit infinitely small by taking the limit of (9) as  $T \rightarrow 0$  (or equivalently  $k \rightarrow \infty$ ). Then,

$$\begin{aligned} \tilde{P} &= \lim_{k \rightarrow \infty} \tilde{P}_k \\ &= \frac{1 - \eta}{1 - \frac{\eta}{1 - \eta} \frac{\delta}{\left( \frac{\mu_i}{\mu_e} \frac{\lambda_1}{\lambda_1 - 1} + 1 \right) \lambda_1^{N+L+1} - \left( \frac{\mu_i}{\mu_e} \frac{\lambda_2}{\lambda_2 - 1} + 1 \right) \lambda_2^{N+L+1}}} \quad (11) \end{aligned}$$

where the auxiliary variables  $\delta$  and  $\lambda_i$  are given in Appendix A.

It is also interesting to consider the case where either the energy storage capacity or the queue capacity is sufficiently large. Then the probability of packet loss becomes

$$\lim_{N \rightarrow \infty \text{ or } L \rightarrow \infty} \tilde{P} = \begin{cases} 1 - \eta & \eta < 1 \\ 0 & \eta > 1 \end{cases}.$$

$$\tilde{P}_k = \frac{p \left( kp - \frac{w}{w+r} \right) \left\{ \frac{[(k-r)(g_{1,k+1}) - g_{1,k}(w+r)(k-1)^2] \lambda_{1,k}^{N+L-2}}{(s_k + g_{1,k}) g_{2,k}} - \frac{[(k-r)(g_{2,k+1}) + g_{2,k}(w+r)(k-1)^2] \lambda_{2,k}^{N+L-2}}{(s_k + g_{2,k}) g_{1,k}} \right\}}{\frac{(-u_{1,k} g_{1,k} + u_{2,k}) \lambda_{1,k}^{N+L-1}}{(1-w-r)(s_k + g_{1,k}) g_{2,k}} + \frac{(u_{1,k} g_{2,k} - u_{2,k}) \lambda_{2,k}^{N+L-1}}{(1-w-r)(s_k + g_{2,k}) g_{1,k}} - \frac{w(1-p)(k-r) \delta_k}{k^2 p(w+p-wp-rp)(s_k + g_{2,k})(s_k + g_{1,k}) g_{1,k} g_{2,k}}} \quad (9)$$

$$\tilde{P}_{k=1, L=0} = \frac{1 - \eta}{1 - \frac{\mu_i}{\mu_a} \left( \frac{\rho}{\mu_e E} - 1 \right) \left[ 1 - \frac{\frac{\rho}{\mu_e E}}{1 + \left( \frac{\rho}{\mu_e E} - 1 \right) \frac{\mu_e}{\mu_i} \frac{\eta}{1-\eta}} \right]^N \left[ 1 - \frac{\mu_i E}{\rho} + \frac{\mu_a E}{\rho \left( \frac{\rho}{\mu_e E} - 1 \right)} \right]^2} \quad (10)$$

This result, which is identical to (8), is of course consistent with basic results from queueing theory. It shows that an energy-harvesting node with infinitely large energy storage or infinitely large queue has zero probability of event loss if the system is over-resourced. This is because in the over-resourced case, the extra energy is continuously stored into the storage and the stored energy increases continuously. In the under-resourced scenario, the unprocessed events are continuously added to the queue and the queue length increases without bound. Thus, if the system is under-resourced, the probability of event loss is equal to the difference between the required consumption power and the harvested power, normalized by the required power.

Another interesting extreme is when the harvesting device is large (i.e.  $\rho$  is large). This case isolates the effect of the limited energy storage capacity on the probability of event loss. The probability of event loss with a large harvesting device can be calculated from (11) as  $\rho$  approaches infinity;

$$\lim_{\rho \rightarrow \infty} \tilde{P} = \frac{\mu_a}{\mu_i + \mu_a} \left( \frac{\mu_e}{\mu_i + \mu_e} \right)^{N+L}. \quad (12)$$

#### IV. AVERAGE DELAY

We saw in (9) and (11) that the probability of event loss is a function of  $N + L$ . Thus, the energy storage capacity and the queue capacity can be freely traded for each other, with no impact on the probability of event loss. On the other hand, the choice of  $L$  and  $N$  matters when the delay before each event is processed is considered.

Using the approximated Markov chain (Appendix A) and Little's formula [38], the approximate average delay is

$$\tilde{D} = \frac{1}{\mu_e(1 - \tilde{P})} \sum_{n=-L}^{-1} -n (\tilde{\pi}_{2(n+L)} + \tilde{\pi}_{2(n+L)+1})$$

which yields (13). Derivation details are given in Appendix B.

It is also interesting to look at the average delay when  $N$ ,  $L$  or  $\rho$  are large. Derivations for the following results are also provided in Appendix B. For a node with sufficiently large  $N$  we have

$$\lim_{N \rightarrow \infty} \tilde{D} = \begin{cases} \frac{L}{\mu_e \eta} - \frac{\lambda_1 - \lambda_1^{1-L}}{\mu_e (\lambda_1 - 1)} & \eta < 1 \\ 0 & \eta > 1 \end{cases}.$$

That is, the average delay is non-zero only if the node is under-resourced. If the node is over-resourced, in the long term the stored energy will increase without bound. Consequently events will be processed immediately without being delayed. However, a node with sufficiently large queue but limited energy storage capacity and harvesting power always has an infinite delay if the node is under-resourced. A sufficiently

large queue will reduce the delay to a finite value if the system is over-resourced:

$$\lim_{L \rightarrow \infty} \tilde{D} = \begin{cases} \infty & \eta < 1 \\ \frac{\eta - 1}{\mu_e \delta} \left[ \frac{\frac{\mu_e E}{\lambda_2 \rho} - 1}{(\lambda_1 - 1)^2} \lambda_1^{N+2} - \frac{\frac{\mu_e E}{\lambda_1 \rho} - 1}{(\lambda_2 - 1)^2} \lambda_2^{N+2} \right] & \eta > 1 \end{cases}$$

It is then easy to see that the average delay for sufficiently large  $N$  and  $L$  is infinite if the node is under-resourced and is zero if the node is over-resourced:

$$\lim_{N, L \rightarrow \infty} \tilde{D} = \begin{cases} \infty & \eta < 1 \\ 0 & \eta > 1 \end{cases},$$

which is quite intuitive and may also be obtained by using results from queueing theory.

When  $\rho$  approaches infinity, since the energy storage capacity is limited, the infinite harvesting power is wasted and only fully charges the storage when harvesting. The average delay depends on the time duration between harvesting cycles and is

$$\lim_{\rho \rightarrow \infty} \tilde{D} = \frac{\left( \frac{\mu_e}{\mu_i + \mu_e} \right)^{N+L} - \left( \frac{\mu_e}{\mu_i + \mu_e} \right)^N}{\mu_i \left( \frac{\mu_e}{\mu_i + \mu_e} \right)^{N+L} - \frac{\mu_i(\mu_i + \mu_a)}{\mu_a}}.$$

However, if the energy storage capacity is also large, the delay is zero regardless of the length of queue (which is always empty). That is

$$\lim_{\rho, N \rightarrow \infty} \tilde{D} = 0.$$

Finally, when both the queue capacity  $L$  and the harvesting power  $\rho$  approach infinity, the average delay exponentially decreases with  $N$ :

$$\lim_{\rho, L \rightarrow \infty} \tilde{D} = \frac{\mu_a}{\mu_i(\mu_a + \mu_i)} \left( \frac{\mu_e}{\mu_e + \mu_i} \right)^N.$$

#### V. SYSTEM DESIGN

We now use the results obtained in the previous section to design the system parameters, given tolerable values of event loss probability,  $P_t$ , and average delay,  $D_t$ . In practice, the harvesting parameters  $\mu_a$  and  $\mu_i$  depend on the characteristics of the energy source and therefore can not be designed. The arrival rate of events depends on the application. In some applications it may be possible to schedule the frequency of events. However, in many applications this is not possible. Therefore, the parameters which one may design are the capacity of the energy storage device,  $N$ , the queue capacity,  $L$ , and the harvesting power,  $\rho$ , (i.e. the size of the harvester).

Assuming linear cost per unit for the energy storage, memory and energy harvester, the total cost is given as  $C(N, L, \rho) = \alpha N + \beta L + \gamma \rho$ , where  $\alpha$ ,  $\beta$  and  $\gamma$  are the unit costs for energy storage, memory and energy harvester,

$$\tilde{D} = \frac{1 - \tilde{P} - \eta}{\mu_e (1 - \tilde{P}) \delta} \left[ \frac{\lambda_1^L - 1}{\lambda_1 - 1} \left( \frac{\mu_i}{\mu_e} \frac{\lambda_1}{\lambda_1 - 1} + 1 \right) \lambda_1^{N+2} - \frac{\lambda_2^L - 1}{\lambda_2 - 1} \left( \frac{\mu_i}{\mu_e} \frac{\lambda_2}{\lambda_2 - 1} + 1 \right) \lambda_2^{N+2} \right] + \frac{L \tilde{P}}{\mu_e (1 - \tilde{P}) (1 - \eta)} \quad (13)$$

respectively. Thus, the design problem can be expressed as the optimization problem

$$\begin{aligned} & \underset{N,L,\rho}{\text{minimize}} && \alpha N + \beta L + \gamma \rho && (14) \\ & \text{subject to} && \mathcal{C}_1 : \tilde{P}(N, L, \rho) \leq P_t \\ & && \mathcal{C}_2 : \tilde{D}(N, L, \rho) \leq D_t, \end{aligned}$$

where  $\tilde{P}(N, L, \rho)$  and  $\tilde{D}(N, L, \rho)$  are given in (11) and (13). We note that the above design problem provides a ‘‘near-optimal’’ solution, since the approximations used in the derivation of (11) and (13) are close.

Since  $\tilde{P}$  is only a function of  $\rho$  and  $M = N + L$ , a simpler form of (14) can be written as

$$\begin{aligned} & \underset{M,L,\rho}{\text{minimize}} && \alpha M + (\beta - \alpha)L + \gamma \rho && (15) \\ & \text{subject to} && \mathcal{C}_1 : \tilde{P}(\rho, M) \leq P_t \\ & && \mathcal{C}_2 : \tilde{D}(\rho, M, L) \leq D_t. \end{aligned}$$

Solving the above optimization problem is not straightforward and requires a three dimensional exhaustive search. However, for the over-resourced case, here we provide an alternative approach that has low complexity, yet it still provides a very good design. Our design procedure is as follows (details are given in Appendix C):

- 1) Solve the single variable optimization problem

$$\begin{aligned} & \underset{\rho}{\text{minimize}} && \omega \log_{\lambda_1} \left[ \frac{\eta \delta P_t}{(1 - \eta) \psi(1 - \eta - P_t)} \right] - \omega + \gamma \rho \\ & \text{subject to} && \eta > 1 \end{aligned}$$

to find  $\rho^\dagger$ , where  $\psi$  is given in (39).

- 2) Find

$$M^\dagger = \log_{\lambda_1} \left[ \frac{\eta \delta P_t}{(1 - \eta) \psi(1 - \eta - P_t)} \right] - 1,$$

where  $\rho^\dagger$  is used to calculate  $\eta$  and  $\delta$ .

- 3) If  $\alpha \leq \beta$ , choose  $N^\dagger = M^\dagger$  and  $L^\dagger = 0$ . If  $\alpha > \beta$ , perform a binary search over  $0 \leq L \leq M^\dagger$  to find the largest  $L$  such that the delay constraint is satisfied.

## VI. NUMERICAL RESULTS

In this section, we validate our theoretical results (11) and (13) by comparing them to simulations. Furthermore, we provide an example for our near-optimal design approach.

### A. Simulation Setup

We have performed continuous-time event-driven simulations using custom written MATLAB<sup>TM</sup> code. The time durations for which the system stays in the active states, inactive states and the time duration between consecutive events are randomly generated and are exponentially distributed with the parameters  $\mu_a$ ,  $\mu_i$ , and  $\mu_e$ , respectively. During the active durations, the harvesting sources harvest energy at rate  $\rho$ . The schedule of event occurrences is also randomly generated. An event is processed (served) over time duration  $\tau$ . That is, the remaining energy in the storage device is gradually decreased at a rate of  $E/\tau$  for a time period  $\tau$ . Events are considered to

be lost if their arrival results in the overflow of the queue. The probability of event loss is calculated as the ratio of the number of lost events and the total number of generated events. The average delay is the mean of the delay for all events, except those lost. The events that are processed immediately without being queued are considered to have a delay of zero.

### B. Simulation Parameters

To choose realistic parameters for our simulations, we consider a MICAz wireless sensor [39] powered by solar energy [40]. In [40], empirically measured solar energy is fitted to a stationary first-order Markovian model, in which the harvested solar energy is quantized into two states with a quantization threshold 1.4mW. Thus, we assume an active harvesting power of  $\rho = 2\text{mW}$  and inactive harvesting power of 0mW in the following simulations. A typical IEEE802.15.4 packet contains data up to 132 bytes [41]. After the data packet is transmitted, an interframe spacing of length equivalent to 16 bytes is used before a 10 byte acknowledgement (ACK) packet is received. The ACK is followed by a 20 byte long interframe spacing before the next transmission. Since the transmission rate is 250Kbps, the total duration of power consumption for one packet is  $(132 + 16 + 10 + 20) \times 8 \text{ bits}/250 \text{ Kbps} = 5.696\text{ms}$ . We assume that each event generates 1320 bytes of data, which requires the transmissions of 10 packets, each 132 bytes long. Thus, the active time period for one single event is  $\tau = 56.96\text{ms}$ . The MICAz sensor [39] operates with a supply voltage from 2.7 ~ 3.3V and its currents are 25.4mA and 27.7mA (including radio power and circuit power) for transmitting at 0dBm and receiving mode, respectively. If we assume that the MICAz sensor is operating with a supply voltage of 3V, the power consumption during transmit and receive modes are 76.2mW and 83.1mW, respectively. Since the transmit power and the receive power are relatively close, we assume that the sensor consumes the power 83.1mW during duration  $\tau$ . Therefore, the energy spent for one event is  $E = 83.1\text{mW} \times 56.96\text{ms} = 4.73\text{mJ}$ .

We assume that a supercapacitor is used as energy storage, since supercapacitors have higher power density and lower energy density than batteries. This means that supercapacitors can deliver the energy to the load faster. Furthermore, supercapacitors can be charged very fast which is a major advantage compared with batteries. A main drawback of supercapacitors is that they are bulky compared with batteries. Therefore, we choose a very small 3F NESSCAP supercapacitor [42], whose energy storage capacity is 3mWh and weighs 1.5g. With these assumptions, a fully-charged energy storage can support  $N = 3 \times 3600 / 4.73 = 2283$  events without recharging. The MICAz sensor has 512KB of flash memory for the measurements [39]. This 512KB memory can hold up to  $L = 512 \times 1000 / (132 \times 10) = 387$  events.

We simulate the two scenarios where  $\mu_a = \mu_i = 1/43200$  Hz and  $\mu_a = \mu_i = 1/3600$ Hz. This means that active-to-inactive or inactive-to-active transition occurs once within 12 hours or once within 1 hour, respectively. The first scenario is meant to model a sunny day when the system stays in the active and the inactive states for about 12 hours each. The

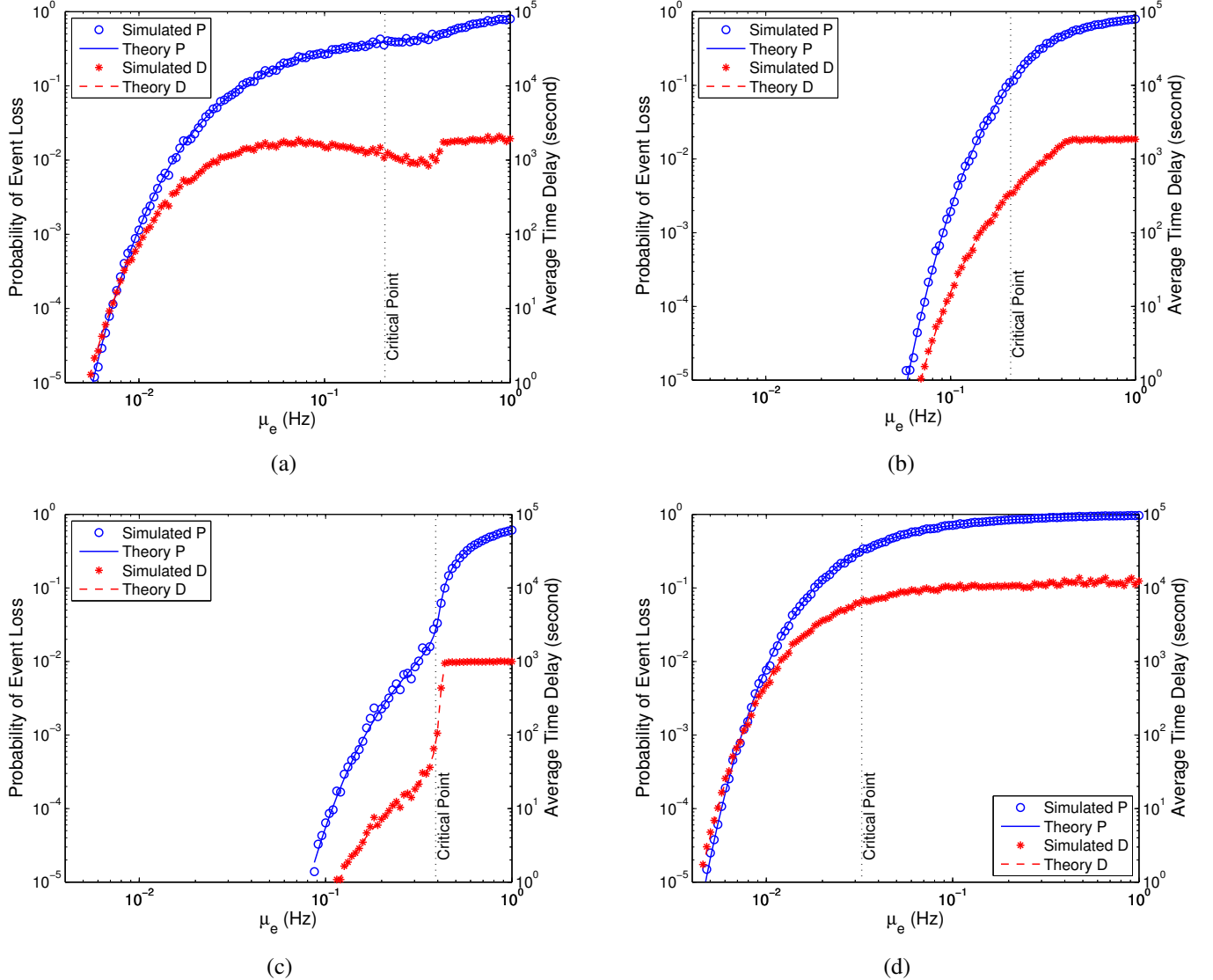


Fig. 2: Comparison of the simulation results and the theoretical approximations of  $P$  and  $D$ . Each event consumes power 83.1mW and operates for 56.96ms. The active harvesting power is  $\rho = 2\text{mW}$ ,  $N = 2281$ ,  $L = 387$  and (a)  $\mu_a = 1/43200\text{Hz}$ ,  $\mu_i = 1/43200\text{Hz}$ , (b)  $\mu_a = 1/3600\text{Hz}$ ,  $\mu_i = 1/3600\text{Hz}$ , (c)  $\mu_a = 1/43200\text{Hz}$ ,  $\mu_i = 1/3600\text{Hz}$ , (d)  $\mu_a = 1/3600\text{Hz}$ ,  $\mu_i = 1/43200\text{Hz}$ .

second scenario is meant to model a partially cloudy day when the active and inactive states are assumed to last roughly 1 hour each. Furthermore, to complete the comparison of the above two scenarios, we simulate two other scenarios where  $\mu_a = 1/43200\text{Hz}$ ,  $\mu_i = 1/3600\text{Hz}$ , and  $\mu_a = 1/3600\text{Hz}$ ,  $\mu_i = 1/43200\text{Hz}$ . These two scenarios are meant to model *fast* and *slow* switching between active and inactive states.

### C. Probability of Event Loss and Average Delay

Fig. 2 compares our theoretical result in (11) and (13), with the simulation results. We can see that the theoretical approximations of  $P$  and  $D$  closely match the corresponding simulation results in most cases. Note the different scales for  $\bar{P}$  and  $\bar{D}$  in the figures, as shown by the left and the right y-axes, respectively. The balanced points of consuming the

exact same energy as harvesting, that is  $\eta = 1$ , are marked by vertical dotted lines in the figures. As shown in Figs. 2(a) and 2(b), the balanced points are the same for the two scenarios  $\mu_a = \mu_i = 1/43200\text{Hz}$  and  $\mu_a = \mu_i = 1/3600\text{Hz}$ . However, the former has a slower harvesting transition between active and inactive states than the latter. Compared to the case in Fig. 2(b), the case in Fig. 2(a) has a full queue during the long inactive periods more often, which implies a larger loss probability and a larger average queueing delay. Fig. 2(c) (Fig. 2(d)) has the smallest (largest) loss probability and the smallest (largest) average queueing delay among all four scenarios. With the same  $\mu_i$ , Fig. 2(b) has larger  $\mu_a$  than Fig. 2(c), which implies a larger balanced point in Fig. 2(c). Furthermore, Fig. 2(d) has the smallest balanced point among the four scenarios, due to its shorter active periods and longer inactive

durations. When the sensor consumes more energy than it harvests (i.e. the under-resourced region on the right of the balanced point),  $\tilde{P}$  and  $\tilde{D}$  have large values. The average queuing delay converges to a fixed value when the queue is always full for relatively larger  $\mu_e$ . When the sensor harvests more energy than it consumes (i.e. the over-resourced region on the left of the balanced point),  $\tilde{P}$  and  $\tilde{D}$  drop sharply to zero for larger  $\mu_i$  in Fig. 2(b) and Fig. 2(c). The falling slope is not too steep for smaller  $\mu_i$  and larger  $\mu_a$  in Fig. 2(d), and is most gradual for smaller  $\mu_i$  and smaller  $\mu_a$  in Fig. 2(a).

As illustrated, a larger probability of event loss corresponds to a larger average delay for most scenarios. The loss probability is close to one at higher  $\mu_e$ , which means that most events are lost instead of waiting in the queue. The average queuing delay is calculated based on the queued events. Thus, the average queuing delay converges to a fixed value at higher  $\mu_e$  when the queue is always full.

#### D. Channel Access

In our analytical calculations we assumed that the energy harvesting sensor processes an event immediately, as long as it has enough energy in its energy storage. In other words, it is implied that the sensor has access to the channel whenever it needs to transmit. In this section, we simulate a more realistic case where access to the channel is not guaranteed. We assume a two-state or “idle/busy” Markovian model for the channel access. The channel is either in the “idle” state, which means that the sensor can access it, or it is in the “busy” state where the sensor cannot access it. The average time durations in the idle (busy) state is denoted by  $T_{\text{idle}}$  (or  $T_{\text{busy}}$ ). Thus, the sensor has channel access with probability  $T_{\text{idle}} / (T_{\text{idle}} + T_{\text{busy}})$ . Fig. 3 compares our proposed model to the simulation results which consider channel access. We can see that the theoretical results closely match those of the simulations, except when  $T_{\text{idle}}$  is quite large.

#### E. System Design

Keeping the same values for  $E$  and  $\rho$ , namely  $E = 4.73\text{mJ}$  and  $\rho = 2\text{mW}$ , we consider the case where the active and the inactive parameters are  $\mu_a = 1/43200\text{Hz}$  and  $\mu_i = 1/43200\text{Hz}$ , and the event arrival rate is one event per 10 minutes, i.e.,  $\mu_e = 1/600\text{Hz}$ . The cost of supercapacitors is roughly  $2.85\$/\text{kJ}$  [43]. If a single event requires energy  $E = 4.73\text{mJ}$ , then the unit cost of energy storage is  $\alpha = 4.73 \times 2.85 \times 10^{-9} = 1.35 \times 10^{-5}\$/\text{event}$ . Currently (in 2012), the list price for a 4GB SD-flash card [44] is approximately  $\$8$ . Thus, we assume that the cost of flash memories is  $\$2/\text{GB}$ . If one event requires ten 132 byte data packets, then the memory cost per queue unit is  $\beta = 1320 \times 2 \times 10^{-9} = 2.64 \times 10^{-6}\$/\text{queue unit}$ . The cost of the solar harvester can be estimated to be  $\gamma = 6\$/\text{W}$  [45]. Using these values we have obtained the optimal solution of the optimization problem (14) using an exhaustive search with a resolution of  $0.01\text{mW}$  for  $\rho$ . Fig. 4 depicts the resulting optimal design parameters  $L^*$ ,  $N^*$ , and  $\rho^*$ , as well as the minimal cost  $C^*$  for different values of  $P_t$  and  $D_t$ . Fig. 4

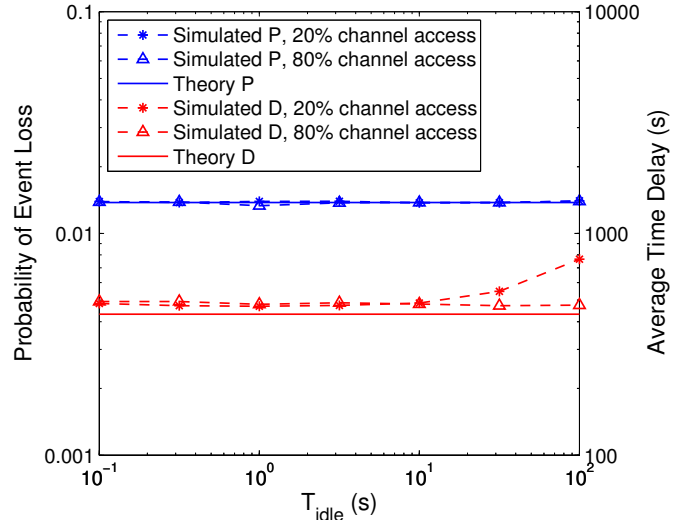


Fig. 3: Comparison of the simulation results and the theoretical approximations of  $P$  and  $D$  with different probabilities of channel access. Each event consumes power  $83.1\text{mW}$  and operates for  $56.96\text{ms}$ . The active harvesting power is  $\rho = 2\text{mW}$ ,  $N = 2281$ ,  $L = 387$ ,  $\mu_a = 1/43200\text{Hz}$ ,  $\mu_i = 1/43200\text{Hz}$ ,  $\mu_e = 1/60\text{Hz}$ .

also provides the design parameters obtained from our near-optimal design approach, namely  $L^\dagger$ ,  $N^\dagger$ , and  $\rho^\dagger$ , as well as the resulting cost  $C^\dagger$ . We can see that the resulting  $L$  and  $N$  are very close. The resulting value of  $\rho$  is also quite close for larger values of  $P_t$ . On the other hand, our near-optimal approach over-designs  $\rho$  by roughly 13%, when  $P_t$  is small. This is of course a consequence of the conservative approach taken while developing the simplified design to ensure that the constraints remain satisfied. However, we see that this over-design of  $\rho$  does not have a noticeable contribution to the overall cost.

## VII. CONCLUSIONS

In this paper we have considered the problem of system design for energy harvesting wireless devices. We have derived closed-form expressions for the probability of event loss and average delay performance metrics for an energy harvesting communication node. To do this, we have constructed a Markov model which combines the energy harvesting process, the event arrival process, the amount of energy remaining in the storage and the number of events queued. Then, based on these analytical results, we have provided a near-optimal design procedure for the capacity of the energy storage and the harvesting device as well as the event queue capacity, given tolerance levels for the probability of event loss and average delay.

### APPENDIX A DERIVATIONS OF EVENT LOSS PROBABILITY

As mentioned in Section II, the inactive states  $(m, 0)$  for  $-Lk \leq m \leq -Lk + k - 1$  lose events since their

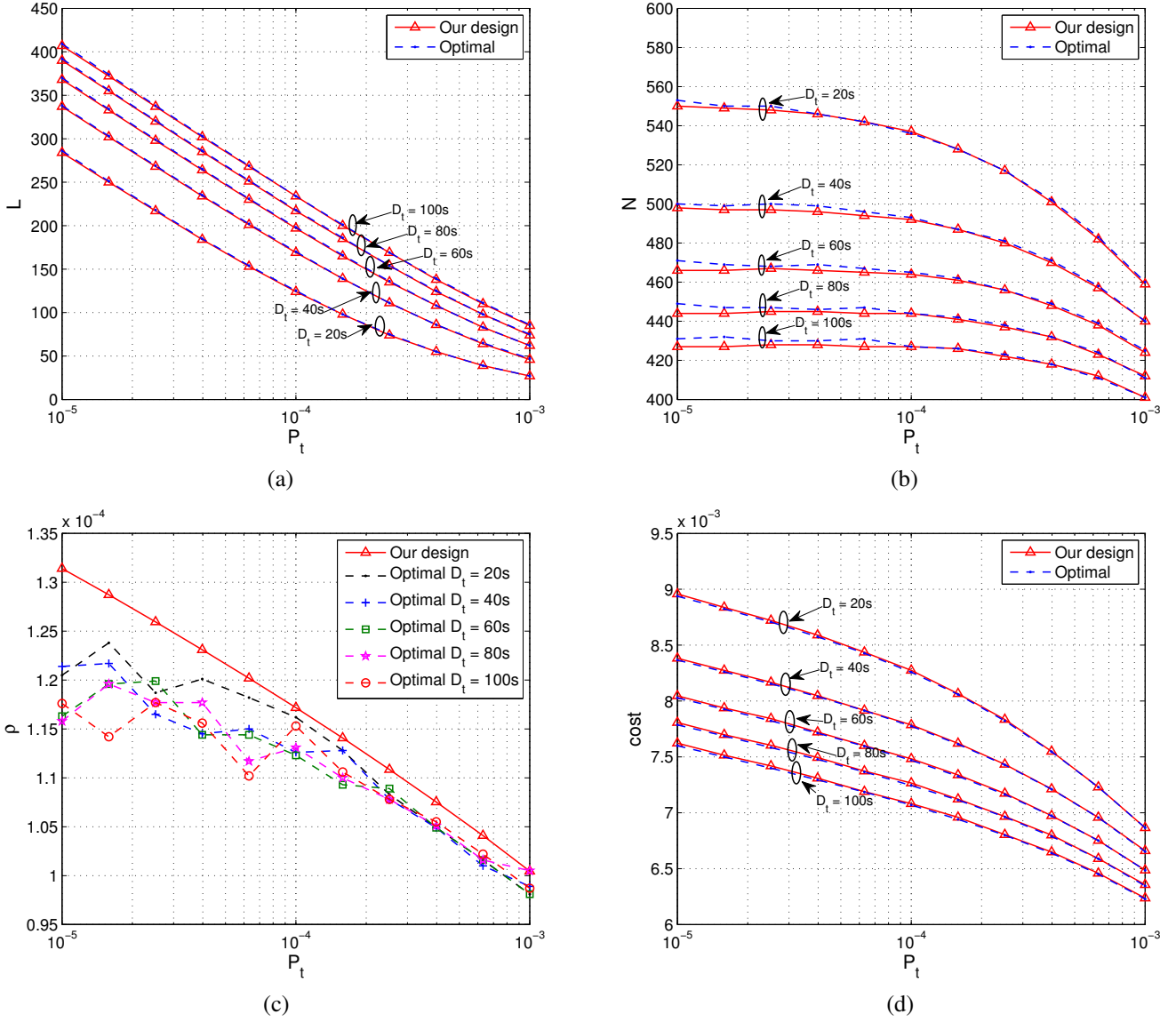


Fig. 4: Comparison of the optimal and the proposed near-optimal design results for (a) the queue capacity  $L$ , (b) the energy storage capacity  $N$ , (c) the harvesting power in active state  $\rho$ , and (d) the total cost of the designed energy harvesting node ( $E = 4.73\text{mJ}$ ,  $\mu_a = 1/43200\text{Hz}$ ,  $\mu_i = 1/43200\text{Hz}$ ,  $\mu_e = 1/600\text{Hz}$ ,  $\alpha = 1.35 \times 10^{-5}\$/\text{energy storage unit}$ ,  $\beta = 2.64 \times 10^{-6}\$/\text{queue unit}$ ,  $\gamma = 6\$/\text{W}$ )

remaining energy is less than  $E$ . Thus, these  $k$  states are merged into a state corresponding to event loss in the inactive state. Similarly, every  $k$  inactive states  $(kn + l, 0)$ ,  $0 \leq l \leq k - 1$ , are merged into a single new state  $(n, 0)$  for each  $-L \leq n \leq N - 1$ , and the last inactive state  $(Nk, 0)$  constitutes the new state  $(N, 0)$  without being merged with any other state. For the active states, the first  $k - 1$  states, i.e.  $(m, 1)$  with  $-Lk \leq m \leq -Lk + k - 2$ , lose incoming events since the combination of their remaining and harvested energies are not enough for supporting an event. Thus, it is reasonable to combine these  $k - 1$  states together to form a new state  $(-L, 1)$ , corresponding to event loss in the active state. Following this, every  $k$  active states  $(kn - 1 + l, 1)$ ,  $0 \leq l \leq k - 1$ , are grouped to a single new state  $(n, 1)$

for each  $-L + 1 \leq n \leq N - 1$ . The last two active states  $(Nk - 1, 1)$  and  $(Nk, 1)$  are combined to a new state  $(N, 1)$ . These groupings are illustrated in Fig. 1. As depicted in Fig. 5, the new Markov model has  $2(N + L + 1)$  states, with the state space  $\{(n, s) | -L \leq n \leq N, s \in \{0, 1\}\}$ . Here,  $n$  denotes the remaining energy in the storage, and  $s$  denotes the energy harvesting state. Note that the number of the original states merged into a new state  $(n, s)$  is  $\Theta(n, s) = k$  for all  $n$  and  $s$ , except for  $\Theta(N, 0) = 1$ ,  $\Theta(N, 1) = 2$  and  $\Theta(-L, 1) = k - 1$ .

Let the transition matrix of the merged Markov chain be denoted as  $\mathbf{Q} = [q_{i,j}]$ , whose entries  $q_{2n+s, 2n'+s'}$  represents the transition probabilities from the state  $(n, s)$  to the state  $(n', s')$ . The transition probability starting from the merged state  $(n, s)$  is averaged over the outgoing probabilities of its

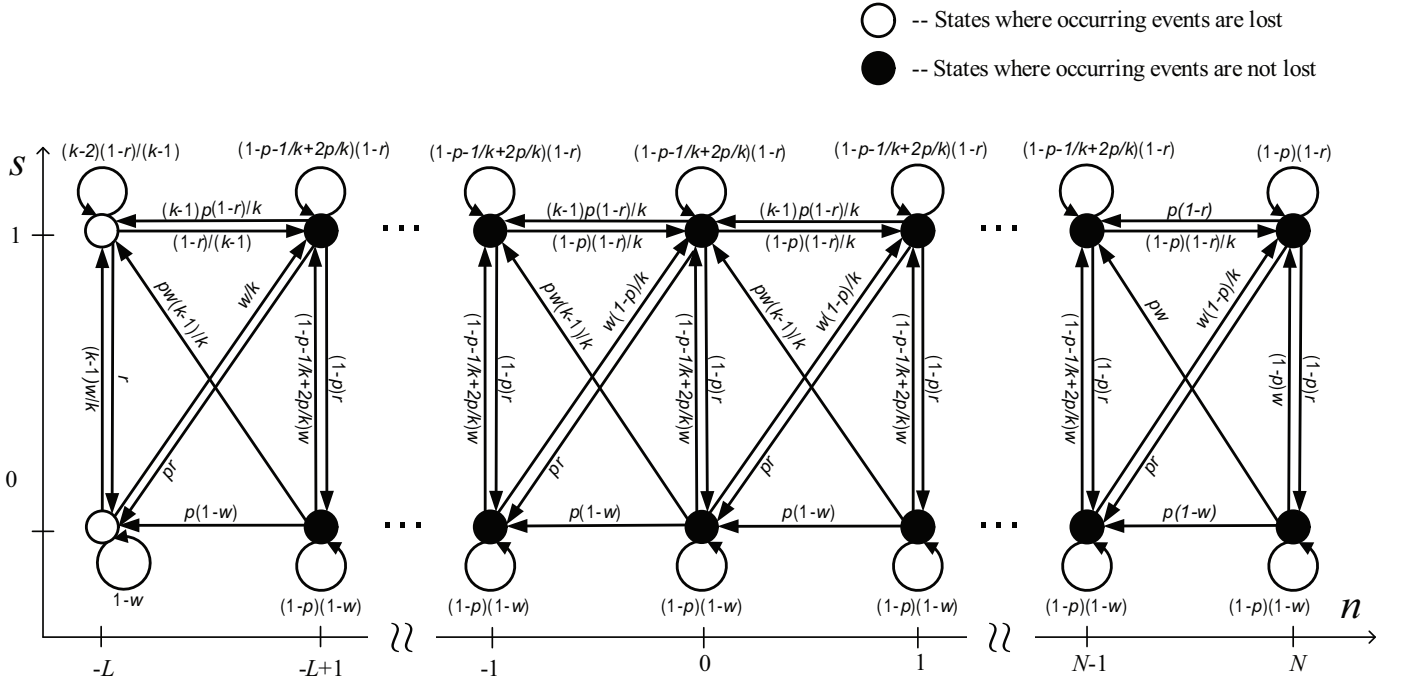


Fig. 5: The merged Markov chain model generated by grouping the states of the original Markov chain model (Fig. 1).

original states  $(m, s)$ , that is

$$= \sum_{m=\max\{nk-s, -Lk\}}^{Q_{2n+s, 2n'+s'}} \sum_{m'=\max\{n'k-s', -Lk\}}^{\min\{(n+1)k-s-1, Nk\} \min\{(n'+1)k-s'-1, Nk\}} \frac{p_{2m+s, 2m'+s'}}{\Theta(n, s)}. \quad (16)$$

If we re-index the states by  $i = 2(n+L) + s$ , using (1)-(5) and (16),  $q_{i,j}$  can be obtained as follows. The states  $i = 0$  and  $i = 1$  are the two states with capability of losing events. Their transition probabilities are

$$q_{0,j} = \begin{cases} 1-w & j=0 \\ \frac{(k-1)w}{k} & j=1 \\ \frac{w}{k} & j=3 \\ 0 & \text{otherwise} \end{cases} \quad (17)$$

and

$$q_{1,j} = \begin{cases} r & j=0 \\ (1-r) \left(1 - \frac{1}{k-1}\right) & j=1 \\ \frac{1-r}{k-1} & j=3 \\ 0 & \text{otherwise} \end{cases}. \quad (18)$$

The states  $i = 2(N+L)$  and  $i = 2(N+L) + 1$ , respectively, have transition probabilities

$$q_{i,j} = \begin{cases} (1-w)p & j=2(N+L)-2 \\ wp & j=2(N+L)-1 \\ (1-w)(1-p) & j=2(N+L) \\ w(1-p) & j=2(N+L)+1 \\ 0 & \text{otherwise} \end{cases} \quad (19)$$

and

$$q_{i,j} = \begin{cases} rp & j=2(N+L)-2 \\ (1-r)p & j=2(N+L)-1 \\ r(1-p) & j=2(N+L) \\ (1-r)(1-p) & j=2(N+L)+1 \\ 0 & \text{otherwise} \end{cases}. \quad (20)$$

For remaining inactive and active states (i.e.  $i \notin \{0, 1, 2N+2L, 2N+2L+1\}$ ) we have

$$q_{i,j} = \begin{cases} (1-w)p & j=i-2 \\ wp \left(1 - \frac{1}{k}\right) & j=i-1 \\ (1-w)(1-p) & j=i \\ w \left(1 - p - \frac{1-2p}{k}\right) & j=i+1 \\ \frac{w(1-p)}{k} & j=i+3 \\ 0 & \text{otherwise} \end{cases} \quad (21)$$

and

$$q_{i,j} = \begin{cases} rp & j=i-3 \\ (1-r)p \left(1 - \frac{1}{k}\right) & j=i-2 \\ r(1-p) & j=i-1 \\ (1-r) \left(1 - p - \frac{1-2p}{k}\right) & j=i \\ \frac{(1-r)(1-p)}{k} & j=i+2 \\ 0 & \text{otherwise} \end{cases}, \quad (22)$$

respectively. Denote the stationary distribution of  $\mathbf{Q}$  as  $\tilde{\pi} = [\tilde{\pi}_0, \tilde{\pi}_1, \dots, \tilde{\pi}_{2(N+L)+1}]^T$  where  $\tilde{\pi}_i$  is the steady-state probability of state  $i$ . The probability of event loss is approximated by  $P_k \simeq \tilde{\pi}_0 + \tilde{\pi}_1 = \tilde{P}_k$ .

In order to simplify the calculation of  $\tilde{\pi}_i$ , we introduce variables  $x_i$ , for  $0 \leq i \leq 2N+1$ , defined by  $x_{2n} = \tilde{\pi}_{2n} + \tilde{\pi}_{2n+1}$  and  $x_{2n+1} = w\tilde{\pi}_{2n} + (1-r)\tilde{\pi}_{2n+1}$ . With this definition we

have  $\tilde{P}_k = x_0$  and  $\sum_{n=0}^{N+L} x_{2n} = 1$ . Moreover, (17)-(22) result in a system of  $2(N+L)+2$  linear equations with variables  $x_i$ , see (23). Inspection of these equations reveals that  $x_{2n}$  and  $x_{2n+1}$  depend on  $x_{2n+2}$  and  $x_{2n+3}$ , for  $0 \leq n \leq N+L-1$ . By iterating this relationship, we get

$$= \begin{cases} \begin{bmatrix} x_{2n} \\ x_{2n+1} \end{bmatrix} \\ \mathbf{BA}^{N+L-2n} \mathbf{C} \begin{bmatrix} s_k \\ 1 \end{bmatrix} x_{2(N+L)+1} & n = 0 \\ \mathbf{A}^{N+L-1-n} \mathbf{C} \begin{bmatrix} s_k \\ 1 \end{bmatrix} x_{2(N+L)+1} & 1 \leq n \leq N+L-1 \\ \begin{bmatrix} s_k \\ 1 \end{bmatrix} x_{2(N+L)+1} & n = N+L \end{cases} \quad (24)$$

where  $s_k = 1 + r/(w+p-wp-rp)$  and

$$\mathbf{A} = \frac{p}{1-p} \begin{bmatrix} \frac{k-(1-p)(k-1)(1-w-r)}{w+p-wp-rp} & -\frac{1}{w+p-wp-rp} \\ k & -1 \end{bmatrix}$$

$$\mathbf{B} = \frac{p}{w} \begin{bmatrix} 1 + \frac{(w+r)(k-1)^2}{k-r} & -1 \\ w + \frac{w(k-1)^2}{k-r} & -w \end{bmatrix}$$

$$\mathbf{C} = \mathbf{A} + \frac{p}{1-p} \begin{bmatrix} 0 & s_k \\ 0 & 1 \end{bmatrix}.$$

Since  $\sum_{n=0}^{N+L} \tilde{\pi}_{2n} = r/(w+r)$  and  $\sum_{n=0}^{N+L} \tilde{\pi}_{2n+1} = w/(w+r)$ , the definition of  $x_i$  yields (25) and (26), where  $\mathbf{A} = \mathbf{VDV}^{-1}$

is the eigen decomposition of  $\mathbf{A}$  and its eigenvalues are

$$\lambda_{1,k} = \frac{p(k-2)}{2(1-p)} + \frac{p[(k-1)r+1+\delta_k]}{2(1-p)(w+p-wp-rp)}$$

and

$$\lambda_{2,k} = \frac{p(k-2)}{2(1-p)} + \frac{p[(k-1)r+1-\delta_k]}{2(1-p)(w+p-wp-rp)},$$

where  $\delta_k = \sqrt{[k(w+p+r-wp-rp)-r-1]^2 + 4(k-1)r}$ .

Solving (26) for  $x_{2(N+L)+1}$  and substituting it in (24) provides all  $x_i$  including (27), where

$$g_{1,k} = -\frac{1}{2} \left[ 1 + \frac{(k-1)r+1+\delta_k}{k(w+p-wp-rp)} \right],$$

$$u_{1,k} = (w+p-wp-rp) [(1-r)(w-k^2p) + wpk(k-1)],$$

$$g_{2,k} = -\frac{1}{2} \left[ 1 + \frac{(k-1)r+1-\delta_k}{k(w+p-wp-rp)} \right],$$

$$u_{2,k} = (1-r) [kp(w+r) - w] + kp^2(k-r)(1-w-r).$$

We can now calculate (27) when  $k$  approaches infinity. Using  $w = \mu_i E/(k\rho)$ ,  $r = \mu_a E/(k\rho)$  and  $p = \mu_e E/(k\rho)$ , we can calculate

$$s = \lim_{k \rightarrow \infty} s_k = 1 + \frac{\mu_a}{\mu_i + \mu_e},$$

$$\delta = \lim_{k \rightarrow \infty} \delta_k = \sqrt{\left[ (\mu_i + \mu_a + \mu_e) \frac{E}{\rho} - 1 \right]^2 + 4\mu_a \frac{E}{\rho}},$$

$$\lambda_1 = \lim_{k \rightarrow \infty} \lambda_{1,k} = \frac{\mu_e \left[ (\mu_i + \mu_a + \mu_e) \frac{E}{\rho} + 1 + \delta \right]}{2(\mu_i + \mu_e)},$$

$$\lambda_2 = \lim_{k \rightarrow \infty} \lambda_{2,k} = \frac{\mu_e \left[ (\mu_i + \mu_a + \mu_e) \frac{E}{\rho} + 1 - \delta \right]}{2(\mu_i + \mu_e)},$$

$$x_i = \begin{cases} \frac{p}{w} \left( 1 + \frac{(w+r)(k-1)^2}{k-r} \right) x_2 - \frac{p}{w} x_3 & i = 0 \\ p \left( 1 + \frac{(k-1)^2}{k-r} \right) x_2 - p x_3 & i = 1 \\ \frac{pk-p(1-p)(k-1)(1-w-r)}{(1-p)(w+p-wp-rp)} x_{i+2} - \frac{p}{(1-p)(w+p-wp-rp)} x_{i+3} & i = 2n, 1 \leq n \leq N+L-2 \\ \frac{pk}{1-p} x_{i+1} - \frac{p}{1-p} x_{i+2} & i = 2n+1, 1 \leq n \leq N+L-2 \\ \frac{pk-p(1-p)(k-1)(1-w-r)}{(1-p)(w+p-wp-rp)} x_{2(N+L)} - \frac{p(1-w-r)}{w+p-wp-rp} x_{2(N+L)+1} & i = 2(N+L)-2 \\ \frac{kp}{1-p} x_{2(N+L)} & i = 2(N+L)-1 \\ \left( 1 + \frac{r}{w+p-wp-rp} \right) x_{2(N+L)+1} & i = 2(N+L) \\ x_{2(N+L)+1} & i = 2(N+L)+1 \end{cases} \quad (23)$$

$$\sum_{n=0}^{N+L} \begin{bmatrix} x_{2n} \\ x_{2n+1} \end{bmatrix} = \{ [(\mathbf{BA}^{-1} + (\mathbf{A} - \mathbf{I})^{-1}) \mathbf{A}^{N+L-1} - (\mathbf{A} - \mathbf{I})^{-1}] \mathbf{C} + \mathbf{I} \} \begin{bmatrix} s_k \\ 1 \end{bmatrix} x_{2(N+L)+1} \quad (25)$$

$$\begin{bmatrix} 1 \\ \frac{w}{w+r} \end{bmatrix} = \{ [(\mathbf{BA}^{-1} + (\mathbf{A} - \mathbf{I})^{-1}) \mathbf{VD}^{N+L-1} \mathbf{V}^{-1} - (\mathbf{A} - \mathbf{I})^{-1}] \mathbf{C} + \mathbf{I} \} \begin{bmatrix} s_k \\ 1 \end{bmatrix} x_{2(N+L)+1} \quad (26)$$

$$\tilde{P}_k = x_0 = \frac{p \left( \frac{w}{w+r} - kp \right) \left\{ \frac{[-(k-r)(g_{1,k+1}) - g_{1,k}(w+r)(k-1)^2] \lambda_{1,k}^{N+L-2}}{(s_k + g_{1,k}) g_{2,k}} + \frac{[(k-r)(g_{2,k+1}) + g_{2,k}(w+r)(k-1)^2] \lambda_{2,k}^{N+L-2}}{(s_k + g_{2,k}) g_{1,k}} \right\}}{\frac{(-u_{1,k} g_{1,k} + u_{2,k}) \lambda_{1,k}^{N+L-1}}{(1-w-r)(s_k + g_{1,k}) g_{2,k}} + \frac{(u_{1,k} g_{2,k} - u_{2,k}) \lambda_{2,k}^{N+L-1}}{(1-w-r)(s_k + g_{2,k}) g_{1,k}} - \frac{w(1-p)(k-r) \delta_k}{k^2 p (w+p-wp-rp) (s_k + g_{2,k}) (s_k + g_{1,k}) g_{1,k} g_{2,k}}} \quad (27)$$

$$\begin{aligned}
g_1 &= \lim_{k \rightarrow \infty} g_{1,k} = -\frac{\lambda_1 \rho}{\mu_e E}, \\
g_2 &= \lim_{k \rightarrow \infty} g_{2,k} = -\frac{\lambda_2 \rho}{\mu_e E}, \\
u_1 &= \lim_{k \rightarrow \infty} u_{1,k} = -\mu_e (\mu_i + \mu_e) \frac{E^2}{\rho^2}, \\
u_2 &= \lim_{k \rightarrow \infty} u_{2,k} = \mu_e^2 \frac{E^2}{\rho^2}.
\end{aligned}$$

Substituting these into (27) yields (28), where  $\eta = \frac{\mu_i \rho}{(\mu_i + \mu_a) \mu_e E}$ . Since  $\mu_i, \mu_a, \mu_e > 0$ , it is easy to verify that  $0 \leq \lambda_2 \leq \frac{\mu_e}{\mu_i + \mu_e}$ . Moreover,  $\lambda_1 > 1$  when  $\eta < 1$ , and  $\frac{\mu_e}{\mu_i + \mu_e} \leq \lambda_1 < 1$  when  $\eta > 1$ . Now, if  $N \rightarrow \infty$  or  $L \rightarrow \infty$ , the limit of (28) becomes

$$\lim_{N \rightarrow \infty \text{ or } L \rightarrow \infty} \tilde{P} = \begin{cases} 1 - \eta & \eta < 1 \\ 0 & \eta \geq 1, \end{cases}$$

and if  $\rho \rightarrow \infty$  we get  $\delta \rightarrow 1 + (\mu_a - \mu_i - \mu_e) \frac{E}{\rho}$ ,  $\lambda_1 \rightarrow \frac{\mu_e}{\mu_i + \mu_e} \left(1 + \frac{\mu_a E}{\rho}\right)$  and  $\lambda_2 \rightarrow 0$ . Thus the probability of event loss for large  $\rho$  can be calculated as

$$\lim_{\rho \rightarrow \infty} \tilde{P} = \frac{\mu_a}{\mu_i + \mu_a} \left( \frac{\mu_e}{\mu_i + \mu_e} \right)^{N+L}.$$

#### APPENDIX B DERIVATIONS OF AVERAGE DELAY

As mentioned in Section IV, the average delay is

$$\tilde{D} = \frac{1}{\mu_e (1 - \tilde{P})} \sum_{n=-L}^{-1} -n x_{2(n+L)}.$$

Using the  $x_i$  (when  $k \rightarrow \infty$ ) calculated in Appendix A, the closed-form solution of the average delay is given by (29), where  $\delta, \lambda_1, \lambda_2$ , and  $\eta$  are given in Appendix A.

Using (29) and recalling that  $0 \leq \lambda_2 \leq \frac{\mu_e}{\mu_i + \mu_e}$  and  $\lambda_1 > 1$  when  $\eta < 1$ , and  $0 \leq \lambda_2 \leq \frac{\mu_e}{\mu_i + \mu_e} \leq \lambda_1 < 1$  when  $\eta > 1$ , the

asymptotic results are readily obtained for  $\tilde{D}$ :

$$\lim_{N \rightarrow \infty} \tilde{D} = \begin{cases} \frac{L}{\mu_e \eta} - \frac{\lambda_1 - \lambda_1^{1-L}}{\mu_e (\lambda_1 - 1)} & \eta < 1 \\ 0 & \eta \geq 1 \end{cases} \quad (30)$$

$$\lim_{L \rightarrow \infty} \tilde{D} = \begin{cases} \infty & \eta < 1 \\ \frac{\eta - 1}{\mu_e \delta} \left[ \frac{(\frac{\mu_e E}{\rho \lambda_2} - 1) \lambda_1^{N+2}}{(\lambda_1 - 1)^2} - \frac{(\frac{\mu_e E}{\rho \lambda_1} - 1) \lambda_2^{N+2}}{(\lambda_2 - 1)^2} \right] & \eta \geq 1 \end{cases} \quad (31)$$

$$\lim_{\rho \rightarrow \infty} \tilde{D} = \frac{\left[ \left( \frac{\mu_e}{\mu_i + \mu_e} \right)^L - 1 \right] \left( \frac{\mu_e}{\mu_i + \mu_e} \right)^N}{\mu_i \left( \frac{\mu_e}{\mu_i + \mu_e} \right)^{N+L} - \frac{\mu_i (\mu_i + \mu_a)}{\mu_a}} \quad (32)$$

$$\lim_{\substack{N \rightarrow \infty \\ L \rightarrow \infty}} \tilde{D} = \begin{cases} \infty & \eta < 1 \\ 0 & \eta \geq 1 \end{cases} \quad (33)$$

$$\lim_{\rho \rightarrow \infty} \tilde{D} = 0 \quad (34)$$

$$\lim_{\substack{L \rightarrow \infty \\ \rho \rightarrow \infty}} \tilde{D} = \frac{\mu_a}{\mu_i (\mu_a + \mu_i)} \left( \frac{\mu_e}{\mu_e + \mu_i} \right)^N. \quad (35)$$

#### APPENDIX C DERIVATIONS OF THE LOW COMPLEXITY DESIGN APPROACH

We focus on the over-resourced case ( $\eta > 1$ ), as this is a more desirable scenario in practice. We take a two step design approach. First, as an approximation, instead of the cost function  $C$ , we consider its upper bound,  $C_u = \omega M + \gamma \rho$ , where  $\omega = \max\{\alpha, \beta\}$ , and perform minimization constrained only to  $\mathcal{C}_1$ . That is, we will first consider

$$\underset{M, \rho}{\text{minimize}} \quad \omega M + \gamma \rho \quad (36)$$

$$\text{subject to } \mathcal{C}_1 : \tilde{P}(\rho, M) \leq P_t.$$

This optimization problem yields  $\rho^\dagger$  and  $M^\dagger = N + L$ . Then, in the second step, we will use constraint  $\mathcal{C}_2$  and costs  $\alpha$  and  $\beta$  to find the best split of  $M^\dagger$  between  $N^\dagger$  and  $L^\dagger$ . That is

$$\underset{L}{\text{minimize}} \quad \alpha(M^\dagger - L) + \beta L \quad (37)$$

$$\text{subject to } \mathcal{C}_2 : \tilde{D}(\rho^\dagger, M^\dagger, L) \leq D_t.$$

$$\begin{aligned}
\tilde{P} &= \lim_{k \rightarrow \infty} \tilde{P}_k = \frac{(\mu_i + \mu_a) \mu_e E - 2\mu_i \rho + \frac{\mu_i^2 \rho^2}{(\mu_i + \mu_a) \mu_e E}}{(\mu_i + \mu_a) \mu_e E - \mu_i \rho - \frac{\mu_i \mu_e \rho \delta (\lambda_1 - 1) (\lambda_2 - 1)}{(\lambda_2 - 1) [(\mu_i + \mu_e) \lambda_1 - \mu_e] \lambda_1^{N+L+1} - (\lambda_1 - 1) [(\mu_i + \mu_e) \lambda_2 - \mu_e] \lambda_2^{N+L+1}}} \\
&= \frac{1 - \eta}{1 - \frac{\frac{\eta}{1-\eta} \delta}{\left[ \frac{\mu_i \lambda_1}{\mu_e (\lambda_1 - 1)} + 1 \right] \lambda_1^{N+L+1} - \left[ \frac{\mu_i \lambda_2}{\mu_e (\lambda_2 - 1)} + 1 \right] \lambda_2^{N+L+1}}}, \quad (28)
\end{aligned}$$

$$\begin{aligned}
\tilde{D} &= \frac{\frac{[(\mu_i + \mu_a) \mu_e E (\lambda_1 - 1) \lambda_1^{L-1} L - \mu_i \rho (\lambda_1^L - 1)] \lambda_1^{N+2}}{\mu_e \mu_i \rho [(\mu_i + \mu_e) \lambda_2 - \mu_e] (\lambda_1 - 1)^2} - \frac{[(\mu_i + \mu_a) \mu_e E (\lambda_2 - 1) \lambda_2^{L-1} L - \mu_i \rho (\lambda_2^L - 1)] \lambda_2^{N+2}}{\mu_e \mu_i \rho [(\mu_i + \mu_e) \lambda_1 - \mu_e] (\lambda_2 - 1)^2}}{\frac{\lambda_1^{N+L+1}}{[(\mu_i + \mu_e) \lambda_2 - \mu_e] (\lambda_1 - 1)} - \frac{\lambda_2^{N+L+1}}{[(\mu_i + \mu_e) \lambda_1 - \mu_e] (\lambda_2 - 1)} - \frac{(\mu_i + \mu_a) \mu_e^2 E \delta}{[(\mu_i + \mu_a) \mu_e E - \mu_i \rho] [(\mu_i + \mu_e) \lambda_1 - \mu_e] [(\mu_i + \mu_e) \lambda_2 - \mu_e]}} \\
&= \frac{L \tilde{P}}{\mu_e (1 - \tilde{P}) (1 - \eta)} - \frac{(\tilde{P} - 1 + \eta)}{\mu_e \delta (1 - \tilde{P})} \left\{ \left[ \frac{\mu_i \lambda_1}{\mu_e (\lambda_1 - 1)} + 1 \right] \frac{(\lambda_1^L - 1) \lambda_1^{N+2}}{\lambda_1 - 1} - \left[ \frac{\mu_i \lambda_2}{\mu_e (\lambda_2 - 1)} + 1 \right] \frac{(\lambda_2^L - 1) \lambda_2^{N+2}}{\lambda_2 - 1} \right\} \quad (29)
\end{aligned}$$

We start by considering (36). It is easy to verify that for over-resourced systems,  $0 \leq \lambda_2 \leq \frac{\mu_e}{\mu_i + \mu_e} \leq \lambda_1 \leq 1$ , which implies  $\frac{\mu_i \lambda_1}{\mu_e (\lambda_1 - 1)} + 1 \leq 0$  and  $\frac{\mu_i \lambda_2}{\mu_e (\lambda_2 - 1)} + 1 \geq 0$ . Thus, if  $M = N + L \geq M_0$ , we have

$$\psi \lambda_1^{N+L+1} \geq - \left[ \frac{\mu_i \lambda_1}{\mu_e (\lambda_1 - 1)} + 1 \right] \lambda_1^{N+L+1} + \left[ \frac{\mu_i \lambda_2}{\mu_e (\lambda_2 - 1)} + 1 \right] \lambda_2^{N+L+1} \quad (38)$$

where

$$\psi = - \left[ \frac{\mu_i \lambda_1}{\mu_e (\lambda_1 - 1)} + 1 \right] + \left[ \frac{\mu_i \lambda_2}{\mu_e (\lambda_2 - 1)} + 1 \right] \left( \frac{\lambda_2}{\lambda_1} \right)^{M_0+1}. \quad (39)$$

Equation (38) provides a better bound if  $M_0$  is larger. To find a good  $M_0$  we recall (12), which is the probability of loss for large  $\rho$ . Thus, we have

$$P_t \geq \tilde{P}(\rho, M) \geq \lim_{\rho \rightarrow \infty} \tilde{P}(\rho, M) = \frac{\mu_a}{\mu_i + \mu_a} \left( \frac{\mu_e}{\mu_i + \mu_e} \right)^M. \quad (40)$$

We can then choose  $M_0$  to be

$$M_0 = \frac{\ln P_t + \ln(\mu_i + \mu_e) - \ln \mu_a}{\ln \mu_e - \ln(\mu_i + \mu_e)} \leq M. \quad (41)$$

Substituting (38) into (11) yields

$$\tilde{P}(\rho, M) \leq \frac{1 - \eta}{1 + \frac{\eta \delta}{(1 - \eta) \psi \lambda_1^{M+1}}} = P_t, \quad (42)$$

where the upper limit of  $\tilde{P}$  is set to the tolerable probability of event loss. Solving (42) for  $M$  yields

$$M = \log_{\lambda_1} \left[ \frac{\eta \delta P_t}{(1 - \eta) \psi (1 - \eta - P_t)} \right] - 1. \quad (43)$$

Now using (43), instead of the optimization problem (36), we can solve

$$\underset{\rho}{\text{minimize}} \quad \omega \left\{ \log_{\lambda_1} \left[ \frac{\eta \delta P_t}{(1 - \eta) \psi (1 - \eta - P_t)} \right] - 1 \right\} + \gamma \rho \quad (44)$$

subject to  $\eta > 1$

which has slightly smaller feasible set. This is a convex minimization problem with a single variable,  $\rho$ , and can be readily solved to yield  $\rho^\dagger$ . Then, given  $\rho^\dagger$ , we can find  $M^\dagger$  from (43).

In the second step we need to find the best split of  $M^\dagger$  between  $N^\dagger$  and  $L^\dagger$ , such that the delay constraint is satisfied. Since  $\tilde{D}$  is a monotonically increasing function of  $L$ , it is easy to distinguish two cases: If  $\alpha \leq \beta$ , the best solution is  $N^\dagger = M^\dagger$  and  $L^\dagger = 0$ . On the other hand, if  $\alpha > \beta$ , the best  $L^\dagger$  can be easily found using a binary search over  $0 \leq L \leq M^\dagger$  such that the delay constraint is satisfied.

## REFERENCES

- [1] H. Karl and A. Willig, *Protocols and Architectures for Wireless Sensor Networks*. John Wiley & Sons, 2005.
- [2] V. Raghunathan, S. Ganeriwal, and M. B. Srivastava, "Emerging techniques for long lived wireless sensor networks," *IEEE Communications Magazine*, vol. 44, no. 4, pp. 108–114, Apr. 2006.
- [3] J. A. Paradiso and T. Starner, "Energy scavenging for mobile and wireless electronics," *IEEE Pervasive Computing*, vol. 4, no. 1, pp. 18–27, Jan. 2005.
- [4] S. Singh, M. Woo, and C. S. Raghavendra, "Power-aware routing in mobile ad hoc networks," in *Proceedings of the 4th annual ACM/IEEE international conference on Mobile computing and networking (MobiCom)*, 1998, pp. 181–190.
- [5] J. M. Rabaey, M. J. Ammer, J. L. da Silva Jr., D. Patel, and S. Roundy, "PicoRadio supports ad hoc ultra-low power wireless networking," *Computer*, vol. 33, no. 7, pp. 42–48, Jul. 2000.
- [6] J. Polastre, J. Hill, and D. Culler, "Versatile low power media access for wireless sensor networks," in *Proceedings of the 2nd international conference on Embedded networked sensor systems (SenSys)*, Nov. 2004, pp. 95–107.
- [7] M. T. Penella, J. Albesa, and M. Gasulla, "Powering wireless sensor nodes: Primary batteries versus energy harvesting," in *Proceedings of 2009 IEEE Instrumentation and Measurement Technology Conference (I2MTC)*, May 2009, pp. 1625–1630.
- [8] C. R. Murthy, "Power management and data rate maximization in wireless energy harvesting sensors," *International Journal of Wireless Information Networks*, vol. 16, no. 3, pp. 102–117, Jul. 2009.
- [9] P. Castiglione, O. Simeone, E. Erkip, and T. Zemen, "Energy-neutral source-channel coding in energy-harvesting wireless sensors," in *Proceedings of the 9th International Symposium on Modeling and Optimization in Mobile, Ad Hoc, and Wireless Networks (WiOpt)*, May 2011, pp. 183–188.
- [10] K. Kar, A. Krishnamurthy, and N. Jaggi, "Dynamic node activation in networks of rechargeable sensors," *IEEE/ACM Transactions on Networking*, vol. 14, no. 1, pp. 15–26, Feb. 2006.
- [11] N. Jaggi, K. Kar, and A. Krishnamurthy, "Near-optimal activation policies in rechargeable sensor networks under spatial correlations," *ACM Transactions on Sensor Networks*, vol. 4, no. 3, pp. 1–36, May 2008.
- [12] B. Medepally and N. B. Mehta, "Voluntary energy harvesting relays and selection in cooperative wireless networks," *IEEE Transactions on Wireless Communications*, vol. 9, no. 11, pp. 3543–3553, Nov. 2010.
- [13] A. Seyedi and B. Sikdar, "Energy efficient transmission strategies for body sensor networks with energy harvesting," *IEEE Transactions on Communications*, vol. 58, no. 7, pp. 2116–2126, Jul. 2010.
- [14] O. Ozel, J. Yang, and S. Ulukus, "Broadcasting with a Battery Limited Energy Harvesting Rechargeable Transmitter," in *Proceedings of the 9th International Symposium on Modeling and Optimization in Mobile, Ad Hoc, and Wireless Networks (WiOpt)*, Princeton, New Jersey, May 2011.
- [15] J. Yang, O. Ozel, and S. Ulukus, "Broadcasting with an energy harvesting rechargeable transmitter," *IEEE Transactions on Wireless Communications*, vol. 11, no. 2, pp. 571–583, Feb. 2012.
- [16] K. Ramachandran and B. Sikdar, "A population based approach to model the lifetime and energy distribution in battery constrained wireless sensor networks," *IEEE Journal on Selected Areas in Communications*, vol. 28, no. 4, pp. 576–586, May 2010.
- [17] V. Sharma, U. Mukherji, V. Joseph, and S. Gupta, "Optimal energy management policies for energy harvesting sensor nodes," *IEEE Transactions on Wireless Communications*, vol. 9, no. 4, pp. 1326–1336, Apr. 2010.
- [18] R.-S. Liu, P. Sinha, and C. E. Koksal, "Joint energy management and resource allocation in rechargeable sensor networks," in *Proceedings of the 29th IEEE International Conference on Computer Communications (INFOCOM)*, Mar. 2010.
- [19] O. Ozel, K. Tutuncuoglu, J. Yang, S. Ulukus, and A. Yener, "Transmission with energy harvesting nodes in fading wireless channels: Optimal policies," *IEEE Journal on Selected Areas in Communications*, vol. 29, no. 8, pp. 1732–1743, Sep. 2011.
- [20] S. Reddy and C. R. Murthy, "Profile-based load scheduling in wireless energy harvesting sensors for data rate maximization," in *Proceedings of 2010 IEEE International Conference on Communications (ICC)*, May 2010, pp. 1–5.
- [21] K. Tutuncuoglu and A. Yener, "Optimum Transmission Policies for Battery Limited Energy Harvesting Nodes," *IEEE Transactions on Wireless Communications*, vol. 11, no. 3, pp. 1180–1189, Mar. 2012.
- [22] B. Devillers and D. Gündüz, "A general framework for the optimization of energy harvesting communication systems with battery imperfections," *Journal of Communications and Networks*, 2012.
- [23] A. Kansal, J. Hsu, S. Zahedi, and M. B. Srivastava, "Power management in energy harvesting sensor networks," *ACM Transactions on Embedded Computing Systems*, vol. 6, no. 4, pp. 32/1–38, Sep. 2007.

- [24] A. Kansal, D. Potter, and M. B. Srivastava, "Performance aware tasking for environmentally powered sensor networks," in *ACM SIGMETRICS Performance Evaluation Review*, vol. 32, no. 1, Jun. 2004, pp. 223–234.
- [25] J. W. Kimball, B. T. Kuhn, and R. S. Balog, "A system design approach for unattended solar energy harvesting supply," *IEEE Transactions on Power Electronics*, vol. 24, no. 4, pp. 952–962, Apr. 2009.
- [26] National Renewable Energy Laboratory (NREL), *National Solar Radiation Data Base*. [Online]. Available: [http://rredc.nrel.gov/solar/old\\_data/nsrdb/](http://rredc.nrel.gov/solar/old_data/nsrdb/)
- [27] A. Seyedi and B. Sikdar, "Modeling and analysis of energy harvesting nodes in body sensor networks," in *Proceedings of the 5th International Summer School and Symposium on Medical Devices and Biosensors (ISSS-MDBS)*, Jun. 2008.
- [28] D. Niyato, E. Hossain, and A. Fallahi, "Sleep and wakeup strategies in solar-powered wireless sensor/mesh networks: Performance analysis and optimization," *IEEE Transactions on Mobile Computing*, vol. 6, no. 2, pp. 221–236, Feb. 2007.
- [29] A. E. Şuşu, A. Acquaviva, D. Atienza, and G. De Micheli, "Stochastic modeling and analysis for environmentally powered wireless sensor nodes," in *Proceedings of the 6th International Symposium on Modeling and Optimization in Mobile, Ad Hoc, and Wireless Networks and Workshops (WiOpt)*, Apr. 2008, pp. 125–134.
- [30] J. Lei, R. Yates, and L. Greenstein, "A generic model for optimizing single-hop transmission policy of replenishable sensors," *IEEE Transactions on Wireless Communications*, vol. 8, no. 2, pp. 547–551, Feb. 2009.
- [31] B. Medepally, N. B. Mehta, and C. R. Murthy, "Implications of energy profile and storage on energy harvesting sensor link performance," in *Proceedings of 2009 IEEE Global Telecommunications Conference (GLOBECOM)*, Nov. 2009.
- [32] V. Joseph, V. Sharma, and U. Mukherji, "Optimal sleep-wake policies for an energy harvesting sensor node," in *Proceedings of 2009 IEEE International Conference on Communications (ICC)*, Jun. 2009, pp. 1–6.
- [33] R. Szweczyk, J. Polastre, A. Mainwaring, and D. Culler, "Lessons from a sensor network expedition," *Wireless Sensor Networks*, pp. 307–322, 2004.
- [34] K. Langendoen, A. Baggio, and O. Visser, "Murphy loves potatoes: Experiences from a pilot sensor network deployment in precision agriculture," in *Proc. IEEE 20th International Parallel and Distributed Processing Symposium*, 2006.
- [35] O. Tickoo and B. Sikdar, "On the impact of IEEE 802.11 MAC on traffic characteristics," *IEEE Journal on Selected Areas in Communications*, vol. 21, no. 2, pp. 189 – 203, feb 2003.
- [36] M. Petrova, J. Riihijarvi, P. Mahonen, and S. LaBell, "Performance study of IEEE 802.15.4 using measurements and simulations," in *IEEE Wireless Communications and Networking Conference (WCNC)*, vol. 1, april 2006, pp. 487 –492.
- [37] A. Seyedi and B. Sikdar, "Modeling and analysis of energy harvesting nodes in wireless sensor networks," in *Proceedings of the 46th Annual Allerton Conference on Communication, Control, and Computing*, Sep. 2008, pp. 67–71.
- [38] L. Kleinrock, *Queueing Systems Volume 1: Theory*. Wiley Interscience, 1975.
- [39] Crossbow Technology Inc., "MICAz: Wireless measurement system." [Online]. Available: [www.xbow.com](http://www.xbow.com)
- [40] C. K. Ho, P. D. Khoa, and P. C. Ming, "Markovian models for harvested energy in wireless communications," in *Proceedings of 2010 IEEE International Conference on Communication Systems (ICCS)*, Nov. 2010, pp. 311–315.
- [41] IEEE Std 802.15.4-2006, "IEEE standard for information technology - telecommunications and information exchange between systems - local and metropolitan area networks - specific requirements - part 15.4: Wireless medium access control (MAC) and physical layer (PHY) specifications," Sep. 2006.
- [42] NESSCAP Energy Inc., "NESSCAP ultracapacitor products." [Online]. Available: [www.nesscap.com](http://www.nesscap.com)
- [43] R. Ball, "Supercapacitors see growth as costs fall," *Electronics Weekly*, Mar. 2006. [Online]. Available: [www.electronicweekly.com](http://www.electronicweekly.com)
- [44] Kingston Technology Corporation, "Datasheet of SDHC card - class 4." [Online]. Available: [www.kingston.com](http://www.kingston.com)
- [45] U.S. Department of Energy, "\$1/W photovoltaic systems: White paper to explore a grand challenge for electricity from solar," Aug. 2010.



**Shenqiu Zhang** (S'06) received a B.Eng. degree in Communications Engineering from Beijing University of Posts and Telecommunications, Beijing, China, in 2004, and M.Eng. and M.Sci. degrees in Electrical Engineering from Memorial University of Newfoundland, St. John's, Canada, in 2008 and from University of Rochester, NY, USA, in 2010, respectively. She is currently working toward a Ph.D degree in the Department of Electrical and Computer Engineering at University of Rochester. Her current research interests include energy harvesting for wireless and body sensor networks and stochastic modeling of energy sources.



**Alireza Seyedi** (S'95-M'04-SM'10) is a Visiting Assistant Professor in the Department of Electrical Engineering and Computer Science at the University of Central Florida. He has been with the department since August of 2012. Prior to that, was at the University of Rochester and at Philips Research North America. He received his PhD and MS degrees from Rensselaer Polytechnic Institute both in Electrical Engineering, in 2004 and 2000, respectively. He received his BS degree, also in Electrical Engineering, from Sharif University of Technology in 1997. His current research interests are in the convergence of communications and control. In particular, he works on control and decision making for networked systems, distributed and decentralized control, dynamics and stochastics of complex networks, control and communication for energy networks and the Smart Grid, decision and control for systems with stochastic sources of energy, energy harvesting for communications and cognitive radios and networks.



**Biplab Sikdar** (S'98-M'02-SM'09) received the B. Tech degree in electronics and communication engineering from North Eastern Hill University, Shillong, India, M. Tech degree in electrical engineering from Indian Institute of Technology, Kanpur and Ph.D in electrical engineering from Rensselaer Polytechnic Institute, Troy, NY, USA in 1996, 1998 and 2001, respectively. He is currently an Associate Professor in the Department of Electrical, Computer and Systems Engineering of Rensselaer Polytechnic Institute, Troy, NY, USA. His research interests include wireless MAC protocols, transport protocols, network security and queuing theory. Dr. Sikdar is a member of Eta Kappa Nu and Tau Beta Pi and is an Associate Editor of the IEEE Transactions on Communications.